

The evolution of virtual water flows in China's electricity transmission network and its driving forces



Chao Zhang ^{a, b, *}, Gang He ^c, Qian Zhang ^{d, **}, Sai Liang ^e, Samuel C. Zipper ^{d, f}, Ru Guo ^{g, h}, Xu Zhao ⁱ, Lijin Zhong ^j, Jiao Wang ^k

^a School of Economics and Management, Tongji University, Shanghai, 200092, China

^b United Nation Environment-Tongji Institute of Environment for Sustainable Development, Tongji University, Shanghai, 200092, China

^c Department of Technology and Society, College of Engineering and Applied Sciences, Stony Brook University, Stony Brook, NY, 11794, USA

^d Department of Civil Engineering, University of Victoria, Victoria, V8P 5C2, Canada

^e State Key Joint Laboratory of Environment Simulation and Pollution Control, School of Environment, Beijing Normal University, Beijing, 100875, China

^f Kansas Geological Survey, University of Kansas, Lawrence, KS, 66047, USA

^g College of Environmental Science and Engineering, Tongji University, Shanghai, 200092, China

^h Shanghai Institute of Pollution Control and Ecological Security, Shanghai, 200092, China

ⁱ Key Laboratory of Integrated Regulation and Resource Development on Shallow Lakes, Ministry of Education, College of Environment, Hohai University, Nanjing, 210098, China

^j Energy Foundation China Office, Beijing, 100004, China

^k World Resources Institute China Office, Beijing, 100027, China

ARTICLE INFO

Article history:

Received 21 February 2019

Received in revised form

5 September 2019

Accepted 7 September 2019

Available online 11 September 2019

Handling editor: Prof. S Alwi

Keywords:

Electricity transmission

Virtual water

Water footprint

Energy-water nexus

Decomposition analysis

ABSTRACT

Long-distance electricity transmissions could transfer water stress associated with electric power generation from the consumption side to the production side. In China, the rapidly growing scale of west-to-east electricity transmission is contributing to rising water stress in the arid northwestern regions. This study investigates the historical evolution and driving forces of virtual water network embodied in inter-provincial electricity transmissions in China during the past decade (2006–2016), measured by both volumetric and stress-weighted water consumption. Results show that electricity production hubs and load centers increasingly diverged in China. Driven by both growing electricity demand in eastern regions and an increasing share of imported electricity, stress-weighted virtual water export from the water-deficient northwestern provinces increased by 120% during the study period. Water efficiency improvements in thermoelectric power generation have offset 35% of the potential growth in total volumetric virtual water transfers, and more than 50% for stress-weighted virtual water transfers. However, the effect of water efficiency improvements has diminished since 2012. Considering China's ambitious plan to boost west-to-east electricity transmissions in the future, increasing the penetration of wind and solar photovoltaic power in electricity mix in northwestern regions should play a more significant role in relieving water stress in major electricity-exporting provinces.

© 2019 Published by Elsevier Ltd.

1. Introduction

China's power industry has experienced tremendous development in the past decade. This is documented not only by rapid expansion of installed capacities and technological changes in

electricity generation (Zhou et al., 2015), but also by the growing ability of large-scale electricity dispatch through national-wide grid networks (Guo et al., 2016b). Inter-provincial electricity transmissions in China grew from 317 TWh in 2006 to 1,130 TWh in 2017 (nearly 2.6 times), much faster than the national total electricity generation which increased by 1.3 times during the same period. Among all inter-provincial electricity transmissions, long-distance transmissions across sub-national regions grew even more rapidly, increasing by 4.2 times from 82 TWh to 424 TWh during 2006–2017 (CEC, 2018). The spatial distribution of power production centers and load centers are increasingly diverged and

* Corresponding author. School of Economics and Management, Tongji University, Shanghai, 200092, China.

** Corresponding author.

E-mail addresses: chao_zhang@tongji.edu.cn, zhangchao03@gmail.com (C. Zhang), zhangqian@uvic.ca (Q. Zhang).

the dispatch distances are becoming longer. For example, the ultra-high voltage (UHV) electricity transmission line connecting Xinjiang Autonomous Region to the Northwest China Grid and the Central China Grid, which was put into operation in 2014, is nearly 2,200 km long (Wei et al., 2018), roughly equivalent to the distance between Beijing and Hong Kong.

In general, a west-to-east electricity transmission pattern has formed in China (Zeng et al., 2016). This is motivated by two factors. First, China's western regions are endowed with abundant energy resources including huge amounts of coal reserves, hydropower resources, and renewable energy resources such as wind (He and Kammen, 2014) and solar (He and Kammen, 2016). However, most of the load centers are located in mega-city agglomerations in eastern coastal regions. The spatial mismatch between energy resources and load centers requires inter-regional electricity transmission (Chen et al., 2014). Second, to relieve the serious air pollution problem in the densely populated urban agglomerations (Liu et al., 2017), the Chinese government has a strong motivation to move new coal-fired power capacities to the coal-abundant and less populated western regions. The Action Plan for Air Pollution Prevention and Control issued by Chinese State Council in 2014 capped coal consumption in the Beijing-Tianjin-Hebei, Yangtze River Delta and Pearl River Delta areas and planned to meet their growing energy demand by importing more electricity rather than building local coal-fired power plants (State Council, 2014). As a result, twelve west-to-east electricity transmission corridors have been constructed and put into operation by the end of 2017 (Wang and Lu, 2018).

The changing spatial distribution of the power industry has important environmental implications. The intended pollution control effect in densely-populated areas is evident as load centers outsource air pollution emissions to electricity exporting provinces (Li et al., 2018), but power industry development in northwestern China is also facing the problem of water scarcity (Zhang et al., 2016b). Thermoelectric power generation competes for freshwater resources with agriculture and domestic users (McMahon and Price, 2011). For example, thermoelectric power is responsible for 55% of the total freshwater withdrawals in the United States (Averyt et al., 2013), more than 20% in most EU nations (Behrens et al., 2017), and nearly 12% in China (Zhang et al., 2018). The impacts of power sector development on water resources (Zhou et al., 2016), as well as the vulnerability of thermoelectric power generation to quantitative and qualitative changes in freshwater resources (van Vliet et al., 2016), have attracted growing research focus worldwide. Stress on freshwater resources caused by thermoelectric power generation could be even more problematic at smaller spatial units if generation capacities are concentrated in arid watersheds. Studies have shown that in many water-scarce catchments in northwestern China, water withdrawals by the expanding coal power industry exceed 60% of local blue water availability (Zhang et al., 2016a). Excessive exploitation can lead to depletion of surface water and groundwater resources and negative socio-economic impacts (Wada et al., 2016).

The mismatch between coal reserves and freshwater resources in China raises concerns regarding potential impacts of power industry development on water resources. Multiple studies have quantified water use (water withdrawal and/or consumption) by thermoelectric power generation in China through bottom-up accounting approaches, focusing on water scarcity impacts (Zhang et al., 2017a), socioeconomic drivers (Zhang et al., 2018), and different future scenarios by 2030 (Zheng et al., 2016) and 2050 (Liao et al., 2016). These studies revealed the spatial distribution of thermoelectric water use and associated water stress based on information of individual power plants or electric generating units (EGUs). The arid northwestern regions are often

highlighted as a concerning hotspot in China's electricity-water nexus.

By introducing the concept of virtual water (Allan, 1998) and water footprints (Hoekstra et al., 2011), electricity transmission networks can be extended to quantify virtual water networks. A number of studies use input-output (IO) analysis to link water use at the generation side to water footprint embodied in electricity consumption, including IO-based life-cycle assessment (Zhang and Anadon, 2013), hybrid life-cycle approach (Feng et al., 2014), and recent application to grey water (Liao et al., 2019). These analyses incorporate full supply chains associated with electricity generation and consumption. However, as a common weakness of IO analysis, electricity transmissions are expressed in monetary units, rather than actual physical flows, which may introduce considerable uncertainties to footprint accounting.

Another group of studies modeled the electricity transmission network in more detail to estimate the embodied virtual water flows. Zhu et al. (2015) developed a node-flow model of China's power system divided into six sub-national grids, and calculated virtual water flows among the six sub-national regions in 2010. Guo et al. (2016a) used the same model and spatial division as Zhu et al. (2015) and extended the time span of the analysis to 2007–2012. Zhang et al. (2017b) refined the analysis by considering the spatial disparities of water resources availability, in which volumetric water consumption for thermoelectric power generation was converted into scarce water using a water stress indicator (WSI). Beyond China, Chini et al. (2018) evaluated the blue and grey virtual water of electricity transfers among power control areas in the United States, a more disaggregated spatial unit than the administrative division of states.

Besides virtual water, electricity transmission models were also used to quantify carbon footprints (Lindner et al., 2013), virtual carbon emissions of electricity consumption (Qu et al., 2018), and its determinants (Wang et al., 2019). An important difference between water and carbon footprint accounting is that water is a highly localized resource, whereas carbon emissions mix rapidly in the atmosphere and therefore have similar effects on global warming regardless of emission location. Geographic variability of water resources and water stress must be incorporated in studies on the virtual water network of electricity transmissions. This study investigates the historical evolution of the virtual water network embodied in inter-provincial electricity transmissions in China during the past decade (2006–2016) based on detailed water use estimates at electric generating unit level and power transmission data at province level. The water footprint analysis is conducted for both volumetric and stress-weighted water consumption (or scarce water consumption) to account for geographic differences in water availability. Compared with previous studies, this analysis has the following key improvements: 1) more accurate high-resolution data of thermoelectric water consumption are used at the generating unit level, 2) stress-weighted water consumption is measured to reflect more realistic water resources deprivation in water-scarce regions, 3) a longer time span is studied to capture important features of scale and structural changes of China's power industry, and 4) driving forces leading to changes of the virtual water network are identified, which have policy implications for relieving water stress in electricity exporting regions.

2. Materials and methods

This analysis models virtual water transfers associated with inter-provincial electricity transmissions (Section 2.1) and then decomposes the drivers of change over the past 10 years (Section 2.2), drawing on numerous existing datasets (Section 2.3).

2.1. Modeling virtual water transfers via inter-provincial electricity transmissions

The national power system is modeled as an inter-linked network composed of provincial electric grids. For each provincial grid, power supply by local plants plus imported electricity from other provinces equals electricity consumption by local users plus electricity export to other provinces. This balance can also be adapted to quantify virtual water transfer embedded in the electricity transmission network, that is, total virtual water inflows from local power generation plus imported electricity equal total virtual water outflows to local users plus exported electricity, as represented by Eq. (1):

$$\begin{aligned} g_i \cdot df_i + \sum_{j:j \neq i} t_{ji} \cdot ef_j &= \left(\sum_{j:j \neq i} t_{ij} + c_i \right) \cdot ef_i \quad \text{for } i \\ &= 1, 2, \dots, n \end{aligned} \quad (1)$$

where subscript i and j represent provinces, g_i is the total net electricity generation by local power plants in province i , c_i is the total local electricity consumption in province i , t_{ji} is the electricity transmission from province j to province i , df_i is the average direct water consumption factor of unit electricity generation in province i , and ef_i is the virtual water consumption factor, or embodied water footprint, of unit electricity supplied in province i . It is assumed that all fluxes of virtual water feeding into a provincial grid from different sources mix, and as a result the virtual water consumption factor of electricity supply to local end-users is the same as electricity export to other provinces.

In order to calculate ef_i based on inter-provincial electricity transmission data, Eq. (1) is re-arranged as Eq. (2):

$$\begin{aligned} g_i \cdot df_i &= \left(\sum_{j:j \neq i} t_{ij} + c_i \right) \cdot ef_i - \sum_{j:j \neq i} t_{ji} \cdot ef_j \\ &= -t_{1i} \cdot ef_1 - \dots - t_{(i-1)i} \cdot ef_{i-1} + \left(\sum_{j:j \neq i} t_{ij} + c_i \right) \cdot ef_i \\ &\quad - t_{(i+1)i} \cdot ef_{i+1} - \dots - t_{ni} \cdot ef_n \end{aligned} \quad (2)$$

Eq. (2) can be expressed as a matrix form comprising all provinces as follows:

$$\widehat{\mathbf{G}} \cdot \mathbf{DF} = \mathbf{T} \cdot \mathbf{EF} \quad (3)$$

where $\widehat{\mathbf{G}}$ is a diagonal matrix composed of the net electricity generation g_i , \mathbf{DF} is a column vector composed of the direct water consumption factor df_i , \mathbf{EF} is a column vector composed of the virtual water consumption factor ef_i , and \mathbf{T} is a re-arranged inter-provincial electricity transmission matrix given by Eq. (4):

$$\mathbf{T} = \left\{ \begin{array}{cccc} \sum_{j:j \neq 1} t_{1j} + c_1 & -t_{21} & \cdots & -t_{n1} \\ -t_{12} & \sum_{j:j \neq 2} t_{2j} + c_2 & \cdots & -t_{n2} \\ \vdots & \vdots & \ddots & \vdots \\ -t_{1n} & -t_{2n} & \cdots & \sum_{j:j \neq n} t_{nj} + c_n \end{array} \right\} \quad (4)$$

The vector of virtual water consumption factor \mathbf{EF} is then calculated through the inverse matrix of \mathbf{T} below:

$$\mathbf{EF} = \mathbf{T}^{-1} \cdot \widehat{\mathbf{G}} \cdot \mathbf{DF} \quad (5)$$

Eq. (5) links the embodied water footprint on the electricity

consumption side to direct water consumption on the electricity production side. In order to trace the origins of consumption-based virtual water, $T^{-1} \cdot \widehat{\mathbf{G}}$ in Eq. (5) can be defined as matrix \mathbf{L} . Each element in the matrix \mathbf{L} , l_{ij} , represents the amount of electricity generation in province j that is ultimately embodied in one unit of final electricity consumption in province i . This coefficient is the complete electricity import coefficient, which differs from direct electricity import because the entire electricity transmission network is included in deriving this coefficient. The role of matrix \mathbf{L} is similar to the Leontief inverse matrix in the monetary input-output analysis which links final consumption to upstream production.

2.2. Decomposition analysis of changes in virtual water transfer

The national total amount of virtual water transfers (TVW) embodied in electricity transmission is the summation of pair-wise virtual water transfer among provinces, which can be expressed as the following Eq. (6):

$$\begin{aligned} \text{TVW} &= \sum_i^n \sum_{j:j \neq i}^n \text{VW}_{ij} = \sum_i^n \sum_{j:j \neq i}^n c_i \cdot l_{ij} \cdot df_j \\ &= \sum_i^n \sum_{j:j \neq i}^n c_i \cdot im_i \cdot sim_{ij} \cdot dft_j \cdot st_j \end{aligned} \quad (6)$$

In this equation, im_i represents the overall proportion of electricity demand in province i that is satisfied by inter-provincial electricity transmission and can be calculated by summing up the complete electricity import coefficients of province i as the following Eq. (7):

$$im_i = \sum_{j:j \neq i} l_{ij} \quad (7)$$

sim_{ij} represents the share of province j in the total complete electricity import in province i , which is calculated as follows:

$$sim_{ij} = \frac{l_{ij}}{im_i} \quad (8)$$

In this study, only the direct water footprint (consumptive freshwater use) of thermoelectric power generation is considered. Due to the ambiguity of system boundary definitions and multiple functions of reservoirs in many cases, reservoir evaporation associated with hydropower generation is not included, nor is the negligible amount of water use by wind power or solar photovoltaic (PV) power generation. The average direct water consumption factors by province are calculated based on thermoelectric water consumption according to Eq. (9):

$$df_j = dft_j \cdot st_j \quad (9)$$

where dft_j is the average freshwater consumption factor of thermoelectric power generation in province j , measured in m^3/MWh ; st_j is the share of thermal power in total electricity generation in province j .

Changes in the overall virtual water transfer between two years can be decomposed into five factors: growth in total electricity consumption (Δc), growth in the share of inter-provincial electricity transmission in meeting local electricity consumption (Δim), changes in the structure of inter-provincial electricity transmission (Δsim), improvements in water efficiency of thermoelectric power generation (Δdft), and changes in electricity mix (Δst). The authors

used the Log-Mean Divisia Index (LMDI) method (Ang, 2005) to conduct a full decomposition on the five factors as Eq. (10):

$$\begin{aligned} \Delta TVW &= TVW^{t_1} - TVW^{t_0} \\ &= \Delta c + \Delta im + \Delta sim + \Delta df + \Delta st \\ &= \sum_i \sum_{j:j \neq i} L(VW_{ij}^{t_1}, VW_{ij}^{t_0}) \cdot \ln\left(\frac{C_i^{t_1}}{C_i^{t_0}}\right) + \dots \\ &\quad \sum_i \sum_{j:j \neq i} L(VW_{ij}^{t_1}, VW_{ij}^{t_0}) \cdot \ln\left(\frac{im_i^{t_1}}{im_i^{t_0}}\right) + \dots \\ &\quad \sum_i \sum_{j:j \neq i} L(VW_{ij}^{t_1}, VW_{ij}^{t_0}) \cdot \ln\left(\frac{sim_{ij}^{t_1}}{sim_{ij}^{t_0}}\right) + \dots \\ &\quad \sum_i \sum_{j:j \neq i} L(VW_{ij}^{t_1}, VW_{ij}^{t_0}) \cdot \ln\left(\frac{df_j^{t_1} t}{df_j^{t_0}}\right) + \dots \\ &\quad \sum_i \sum_{j:j \neq i} L(VW_{ij}^{t_1}, VW_{ij}^{t_0}) \cdot \ln\left(\frac{st_j^{t_1}}{st_j^{t_0}}\right) \end{aligned} \quad 10$$

The operator $L(VW_{ij}^{t_1}, VW_{ij}^{t_0})$ is defined as follows:

$$L(VW_{ij}^{t_1}, VW_{ij}^{t_0}) = \begin{cases} \frac{VW_{ij}^{t_0} - VW_{ij}^{t_1}}{\ln VW_{ij}^{t_0} - \ln VW_{ij}^{t_1}} & \text{for } VW_{ij}^{t_1} \neq VW_{ij}^{t_0} \\ VW_{ij}^{t_1} & \text{for } VW_{ij}^{t_1} = VW_{ij}^{t_0} \end{cases} \quad 11$$

Some provinces were first connected with other provinces during the study period, for example, Xinjiang began to export electricity in 2010. In such situations, the values of VW_{ij} and sim_{ij} change from 0 to a positive number from t_0 to t_1 and the new virtual water transfer between two provinces (ΔVW_{ij}) was attributed entirely to the structural changes of inter-provincial electricity transmission (Δsim).

2.3. Data

The time span of this study is 2006–2016, during which China's power industry has experienced rapid growth. Two groups of data are used in this study: 1) electricity generation, consumption and transmission data; and 2) water consumption data of thermoelectric power generation. Electricity generation data by fuel and by province in each year are reported in the China Electricity Yearbook (Editorial Board, 2015). Average in-plant auxiliary power consumption ratios by fuel and by province in each year are reported in the Annual Compilation of Statistics of Power Industry in China (CEC, 2000–2015). The net electricity output, which is the actual amount of electricity feeding into the grids, is calculated by subtracting in-plant auxiliary power consumption from electricity generation. Pair-wise inter-provincial electricity transmissions are also reported in the annual compilation of statistics. This study assigns transmission losses to electricity end-users. Electricity consumption by province is calculated through the balance relationship between local electricity production and consumption, and electricity import and export.

This study covers 30 province-level jurisdictions in mainland China. Tibet Autonomous Region is excluded, because it has very little electricity production and consumption and its power grid is not connected to other provinces. The Inner Mongolia Autonomous Region power grid is divided into eastern and western parts which are analyzed separately in this study. The eastern Inner Mongolia grid is operated by State Grid Corporation of China and belongs to the Northeast China Grid branch. The western Inner Mongolia grid is independently operated by a local company.

This study uses a bottom-up time-series water use inventory for China's thermal power industry developed by Zhang et al. (2018). This inventory covers about 99% of China's thermal power capacity; the remaining 1% is mostly small plants under 6 MW that are used by nearby consumers and barely impact the import and export results. It was compiled based on technological information at EGU level and time-series water withdrawal and consumption factors estimated from samples of Chinese power plants. Water consumption within individual EGUs or power plants in this inventory is aggregated to the provincial level to calculate the average water consumption factors of thermoelectric power generation by province.

It is important to distinguish water consumption in water-abundant regions and water-scarce regions, since the same volume of physical water use could have much larger environmental and social impacts in water-scarce regions. For this purpose, the water stress index (WSI) defined by Pfister et al. (2009) is used to

adjust the volumetric water consumption into stress-weighted volume of water consumption. The WSI indicator is based on the concept of water deprivation, which means in river basins under higher water stress, one unit of water use deprives water availability to other users in the same basin to a higher degree. This indicator is calculated by transforming the withdrawal-to-availability ratio into a number between 0 and 1 by an S-shaped curve function as follows:

$$WSI = \frac{1}{1 + e^{-6.4 \cdot WTA} \left(\frac{1}{0.01} - 1 \right)} \quad 12$$

The basic spatial unit for calculating WSI is the 1,120 catchments in China. Withdrawal-to-availability (WTA) ratios by catchment are derived from an updated Aqueduct Baseline Water Stress Map for China in 2010 developed by the World Resources Institute (Wang et al., 2016). Then, the stress-weighted water consumption is calculated by individual EGU or power plant by multiplying the volumetric water consumption by the corresponding WSI value of the catchment where the EGU is located. Based on the exact geographic location of all thermal power plants, the average WSI and electricity generation at plant level is presented for each province in Fig. 1.

3. Results

This study reveals electricity production and consumption in China has increasingly diverged (Section 3.1), as have virtual water

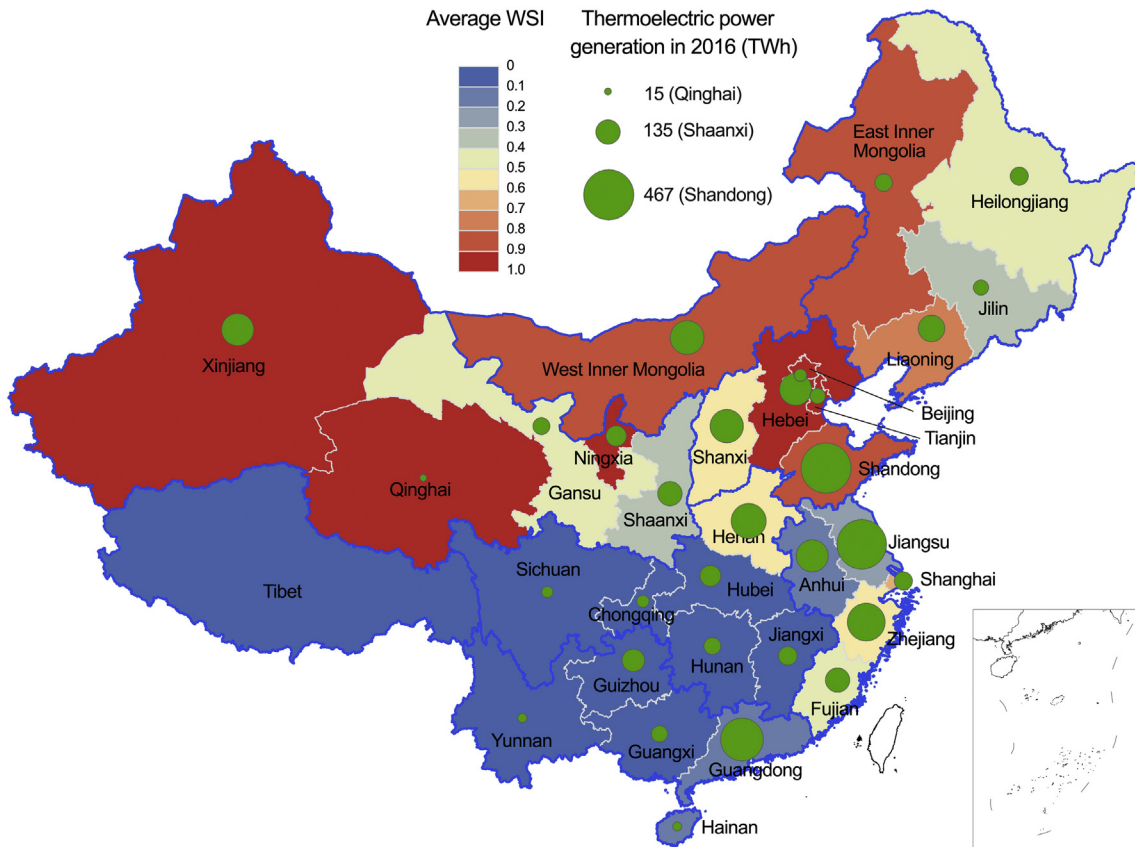


Fig. 1. Spatial distribution of weighting average WSI and thermoelectric power generation by provincial grid. Bold blue lines represent boundaries of regional grids; thin white lines represent provincial boundaries. (For interpretation of the references to color in this figure legend, the reader is referred to the Web version of this article.)

transfers embodied in electricity transmission (Section 3.2). Effects from multiple driving forces are summarized in Section 3.3.

3.1. Increasingly diverged electricity production and consumption in China

China's power industry experienced rapid growth during the study period. The total installed capacity of power generation more than doubled, from 624 GW in 2006 to 1,651 GW in 2016, sustaining a growth of electric power output from 2,850 TWh to 6,023 TWh. Thermal power, including all combustible fuels (fossil fuels, biomass, municipal solid wastes, etc.) and nuclear power, contributed 75.4% of the total power generation in 2016. Along with soaring electricity demand and supply, the spatial distribution of electricity consumption and production has also been changing in China. The most notable trend is the increasing separation of electricity load centers and production centers, which leads to fast growing amounts of inter-provincial electricity transmission. As shown in Fig. 2, inter-provincial electricity transmission experienced a three-fold growth, which is much faster than the two-fold growth of total electricity production. Inter-provincial transmission's share in the national total net electricity production increased from 11.3% in 2006 to 15.9% in 2016.

In general, China has a west-to-east electricity transmission pattern. The more developed eastern coastal regions with higher population density, larger economic output, but fewer energy resources, are major electricity importers. Three mega-city agglomerations are located in the coastal regions, including Beijing-Tianjin-Hebei, Yangtze River Delta (including Shanghai, Jiangsu and Zhejiang), and Pearl River Delta (located in Guangdong). The

gaps between local electricity production and demand in these provinces increased significantly. As shown in Fig. 3, net electricity import doubled in the Beijing-Tianjin-Hebei area (from 76 TWh in 2006 to 162 TWh in 2016), more than tripled in Guangdong (from 50 TWh to 183 TWh) and increased by 4.6 times in the Yangtze River Delta area (from 46 TWh to 212 TWh). Additionally, Shandong became a large electricity importer after 2010, when the Ningxia-

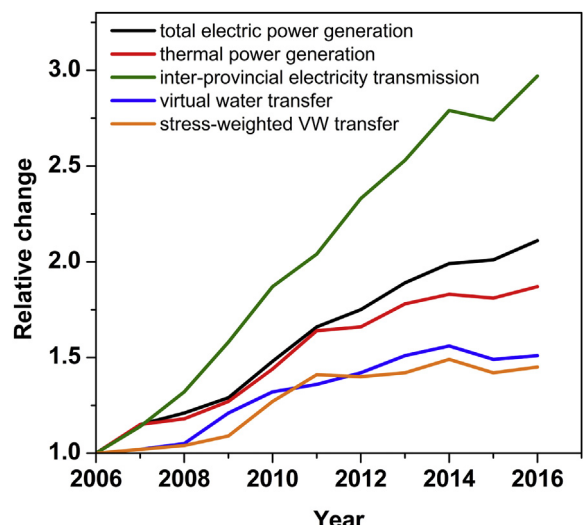


Fig. 2. Relative changes in electric power generation, electricity transmission and virtual water transfer.

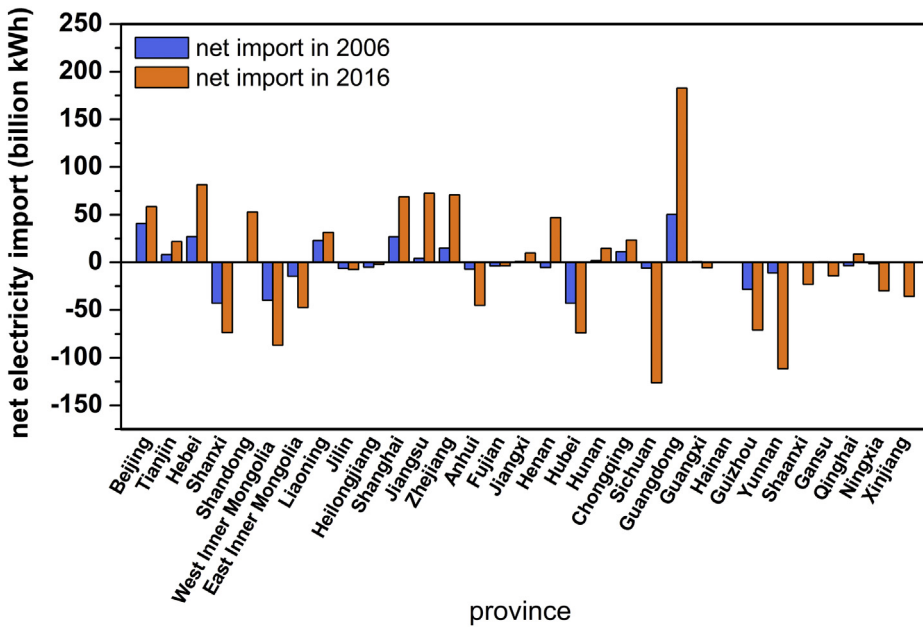


Fig. 3. Growth in inter-provincial electricity transmissions. Negative net import indicates net export. Province abbreviations are explained in Supplementary Materials.

Shandong UHV electricity transmission line was put into commission. These eight provinces (or province-level municipalities) accounted for 82% of the net electricity imports of all provinces.

On the exporting side, all major electricity exporters are located in inland western China. These provinces can be divided into two groups based on different electricity mix. One group includes the northwestern provinces, which are dominated by coal-fired power generation and supplemented by wind and solar PV power. Net electricity export from Shanxi, West Inner Mongolia and East Inner Mongolia increased by 72%, 119% and 224%. These regions have become China's major coal mining areas since the early 2000s. Shaanxi, Gansu, Ningxia and Xinjiang are emerging energy production hubs in which rich coal reserves as well as wind and solar energy resources are under rapid development. They have become new exporters since 2010, and their net electricity export added up to 103 TWh in 2016. The second group includes some southwestern and central provinces where hydropower makes a great contribution. Total net export from Hubei, Sichuan, Yunnan, and Guizhou grew from 88 TWh in 2006 to 383 TWh in 2016. Sichuan is the largest exporter (126 TWh in 2016) in all provinces and has the highest growth rate as well.

With increasing amounts of inter-provincial transmission, importing provinces became less self-sufficient in electricity while exporting provinces had higher degrees of surplus production. The authors define a self-sufficient ratio of electricity for a province as the ratio of local electricity generation over local electricity consumption. The average self-sufficient ratio of electricity in importing provinces decreased from 0.86 to 0.77 (Fig. 4). Three municipalities, Beijing (0.42), Shanghai (0.55) and Tianjin (0.72), had the lowest self-sufficient ratio. The export ratio is defined as the ratio of net electricity export over local electricity generation in exporting provinces. The average electricity export ratio increased from 0.15 to 0.23. Half of the electricity production in West Inner Mongolia is exported. Yunnan, Guizhou and Sichuan also have large export ratios around 0.4.

3.2. Virtual water transfer embodied in electricity transmission

The total volume of virtual water transfer increased by a factor of

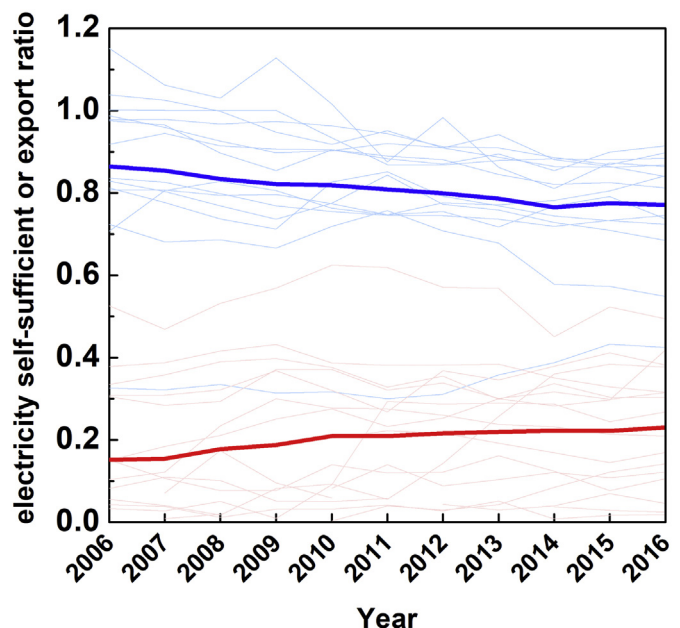


Fig. 4. Changes in electricity self-sufficient ratio in importing provinces (blue lines) and electricity export ratio in exporting provinces (red lines). Bold blue and red lines represent average self-sufficient ratio and export ratio. Light blue and red lines represent each individual province. (For interpretation of the references to color in this figure legend, the reader is referred to the Web version of this article.)

1.5, from $4.84 \times 10^8 \text{ m}^3$ in 2006 to $7.29 \times 10^8 \text{ m}^3$ in 2016. When adjusting volumetric water consumption into stress-weighted water consumption using WSI indicators, virtual scarce water transfer increased from $2.20 \times 10^8 \text{ m}^3$ in 2006 to $3.19 \times 10^8 \text{ m}^3$ in 2016, a factor of 1.45. Proportionally, both volumetric virtual water and stress-weighted virtual water transfers increased more slowly than electricity transmission (Fig. 2). This is mainly attributed to water conservation efforts in China's thermal power industry, which will be further analyzed in the following section 3.3.

Similar to the spatial pattern of electricity transmission, the

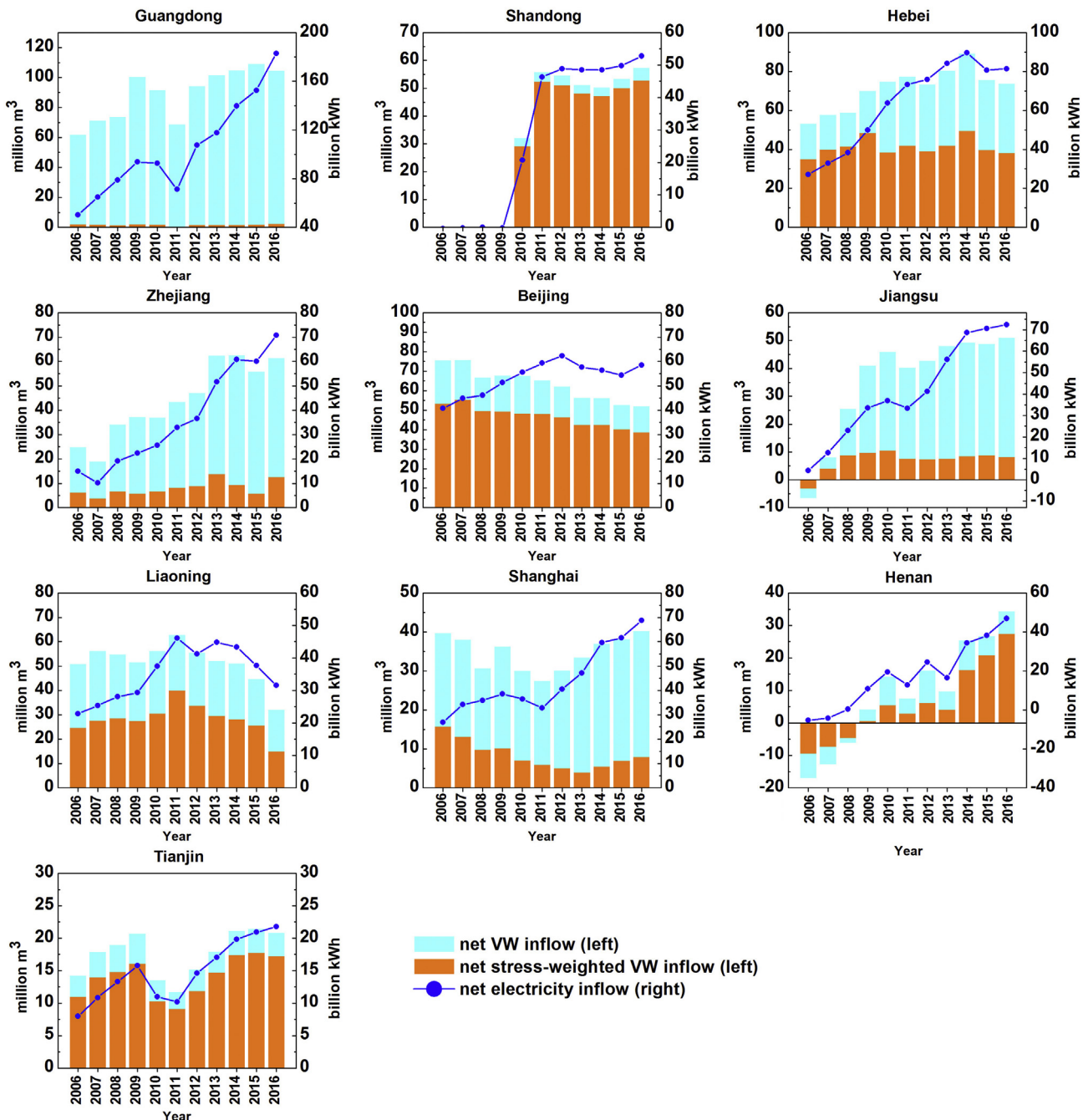


Fig. 5. Trends of net electricity import and virtual water inflow in the top ten provinces. Columns for stress-weighted virtual water (orange) overlap with columns for volumetric virtual water (light blue). (For interpretation of the references to color in this figure legend, the reader is referred to the Web version of this article.)

embodied virtual water transfer also generally follows a west-to-east pattern. Due to different water stress levels and electricity mix in northwestern China and southwestern China, the differences between virtual water and scarce virtual water are evident. Scarce water accounts for very large proportions of virtual water inflows to the Beijing-Tianjin-Hebei region and outflows from northwestern provinces, but very small proportions in inflows to the Yangtze River Delta region and Guangdong and outflows from southwestern provinces (Fig. 5).

Guangdong has the largest virtual water inflow of all provinces at around $100 \times 10^6 \text{ m}^3$ in recent years (Fig. 5). However, since imported electricity to Guangdong mainly comes from the Guizhou,

Yunnan, and Hubei regions which have very low water stress levels (and a correspondingly low WSI), scarce water accounted for a negligible proportion (~2%). Net virtual water inflows to Shanghai, Jiangsu and Zhejiang were around $40-60 \times 10^6 \text{ m}^3$ in recent years. Significant increases occurred in both Jiangsu and Zhejiang. The proportions of scarce water are also low (~20%) in these regions because most imported electricity comes from Hubei and Sichuan, two western hydropower production hubs. The Beijing-Tianjin-Hebei area imports virtual water mainly from West Inner Mongolia and Shanxi, the two largest coal power production hubs in western China. The shares of scarce water in virtual water import are considerably higher in this region, about 75% in Beijing, 80% in

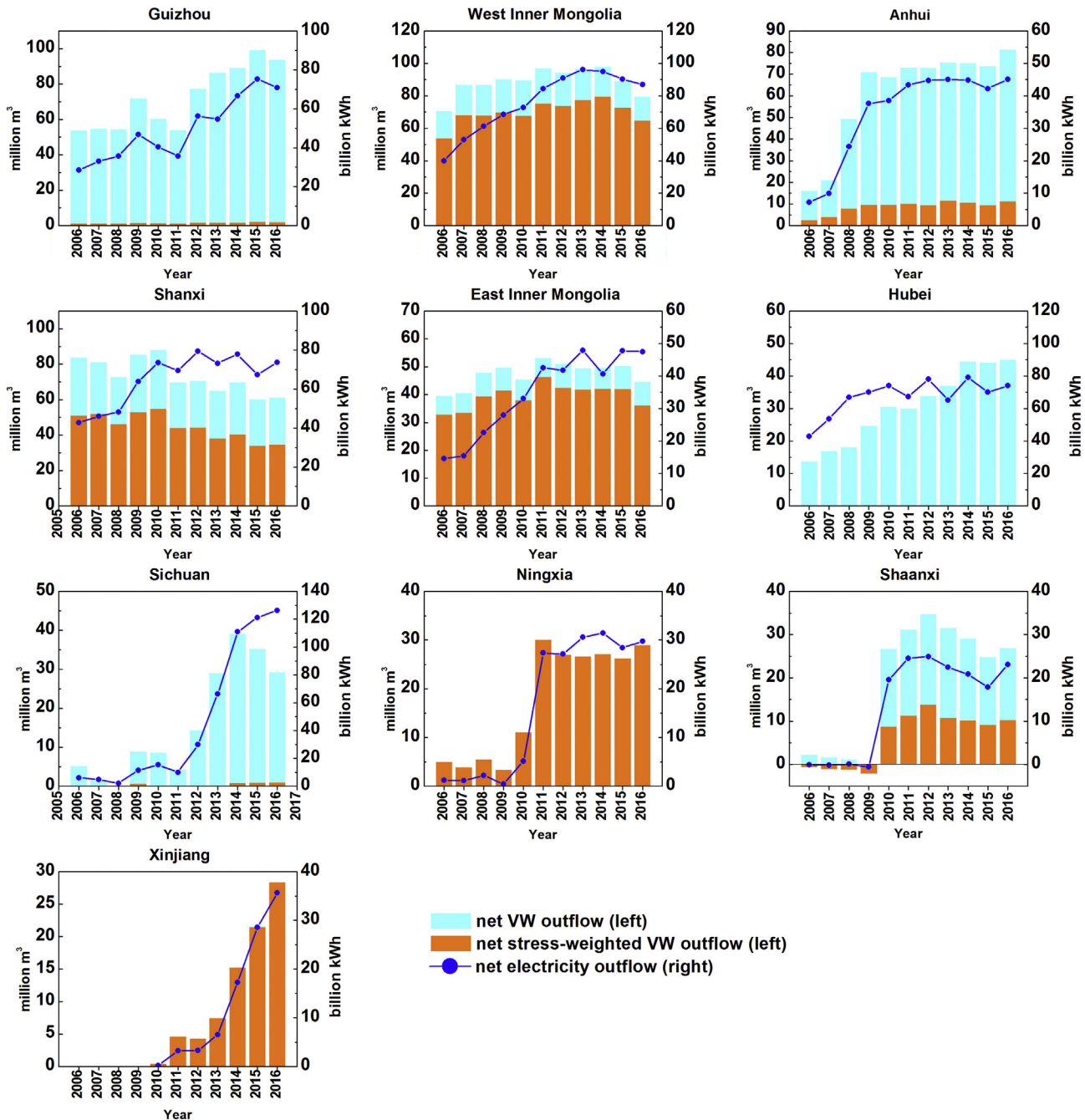


Fig. 6. Changes in net electricity export and virtual water outflow in the top ten provinces. Columns for stress-weighted virtual water (orange) overlap with columns for volumetric virtual water (light blue). (For interpretation of the references to color in this figure legend, the reader is referred to the Web version of this article.)

Tianjin and 50% in Hebei. Notably, net virtual water inflows to Beijing followed a declining trend, from $75 \times 10^6 \text{ m}^3$ in 2006 to $52 \times 10^6 \text{ m}^3$ in 2016, mainly caused by decreasing water intensity in exporting provinces. Shandong province, which imports electricity from Ningxia, has the largest virtual scarce water inflow (around $50 \times 10^6 \text{ m}^3$ after 2011) among all provinces. During the study period, the Henan province in the Central China Grid changed from a net virtual water exporter into a net importer. Both volumetric and stress-weighted virtual water inflows increased quickly after 2014, as it imported water primarily from Xinjiang.

On the exporting side (Fig. 6), central and southwestern provinces, including Guizhou, Hubei, and Sichuan, have quite large

virtual water exports ($93.5 \times 10^6 \text{ m}^3$ in Guizhou, $44.9 \times 10^6 \text{ m}^3$ in Hubei, and $29.2 \times 10^6 \text{ m}^3$ in Sichuan in 2016). Due to their rich water resources endowments and correspondingly low WSI, exporting electricity does not pose pressures on local water availability. On the other hand, a large amount of newly built thermal power capacity is located in northwestern provinces under high water stress. Scarce water accounts for more than 80% in virtual water outflows in West Inner Mongolia and East Inner Mongolia, and nearly 100% in Ningxia and Xinjiang. Xinjiang also experienced the most rapid growth of scarce virtual water export in recent years, from no export in 2009 to $28.4 \times 10^6 \text{ m}^3$ in 2016, compared to the decreasing or stabilized trends in many other exporting

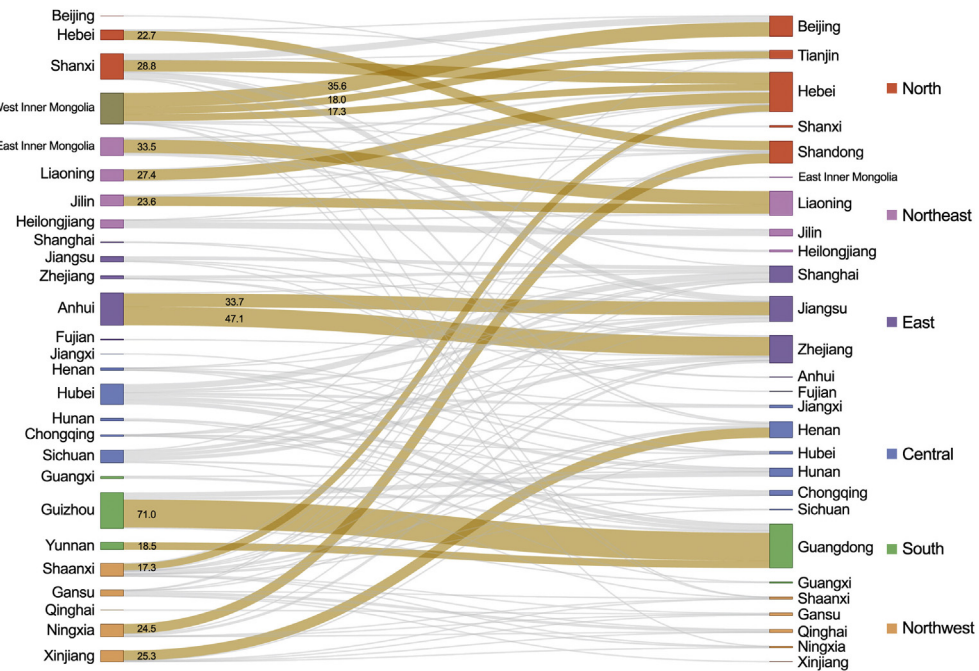


Fig. 7. Pair-wise inter-provincial volumetric virtual water transfers in 2016. Provinces are classified into sub-national grids distinguished by different colors. The fifteen largest flows are highlighted with their amount marked, measured in million m^3 . (For interpretation of the references to color in this figure legend, the reader is referred to the Web version of this article.)

provinces.

The structure of pair-wise inter-provincial volumetric virtual water and stress-weighted virtual water transfers in 2016 are illustrated in Fig. 7 and Fig. 8, respectively. The five largest inter-provincial volumetric virtual water flows are Guizhou-to-Guangdong ($71.0 \times 10^6 \text{ m}^3$), Anhui-to-Zhejiang ($47.1 \times 10^6 \text{ m}^3$),

West Inner Mongolia-to-Beijing ($35.6 \times 10^6 \text{ m}^3$), Anhui-to-Jiangsu ($33.7 \times 10^6 \text{ m}^3$), and East Inner Mongolia-to-Liaoning ($33.5 \times 10^6 \text{ m}^3$). These five pair-wise flows combine to account for 30% of all volumetric virtual water transfers (Fig. 7).

The structure of stress-weighted virtual water transfers differs substantially from its volumetric counterpart (Fig. 8). Northern

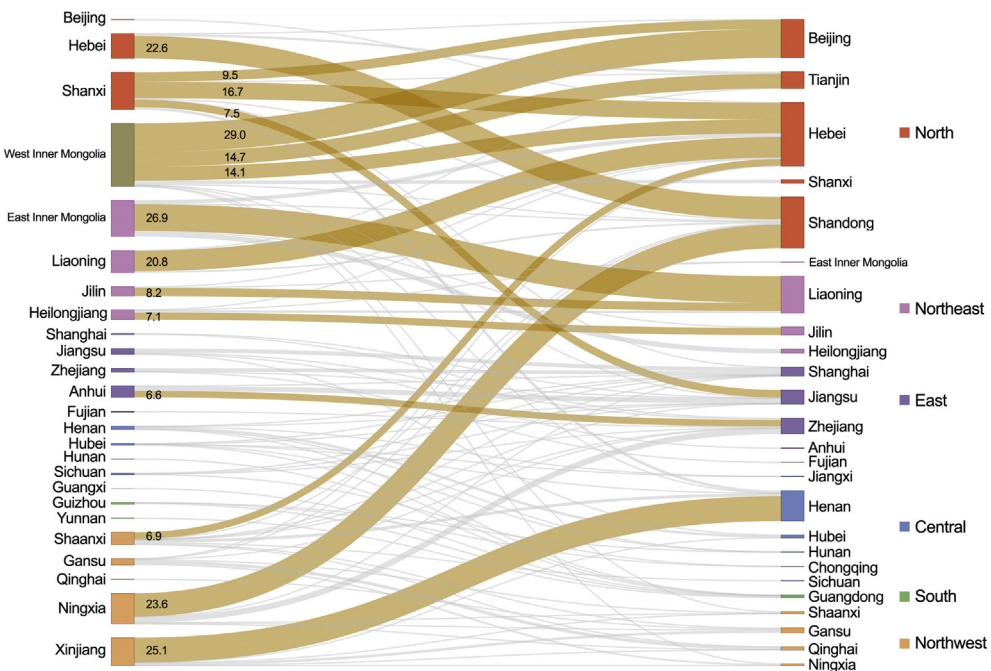


Fig. 8. Pair-wise inter-provincial stress-weighted virtual water transfers in 2016. Provinces are classified into sub-national grids distinguished by different colors. The fifteen largest flows are highlighted with their amount marked, measured in million m^3 . (For interpretation of the references to color in this figure legend, the reader is referred to the Web version of this article.)

provinces dominate the stress-weighted virtual water network. The top five stress-weighted flows are West Inner Mongolia-to-Beijing ($29.0 \times 10^6 \text{ m}^3$), East Inner Mongolia-to-Liaoning ($26.9 \times 10^6 \text{ m}^3$), Xinjiang-to-Henan ($25.1 \times 10^6 \text{ m}^3$), Ningxia-to-Shandong ($23.6 \times 10^6 \text{ m}^3$), and Hebei-to-Shandong ($22.6 \times 10^6 \text{ m}^3$). In the stress-weighted network the role of water-rich southern provinces is smaller compared to the volumetric network. The five largest pair-wise flows account for 40% of total stress-weighted flows in the stress-weighted virtual water network. Aggregated to the regional level, North China Grid is the biggest receiver of scarce water resources via importing electricity, and Northwest China Grid (including West Inner Mongolia) is the biggest exporter.

Northwestern and southwestern provinces are both large electricity exporters, but the impacts of exporting electricity relative to local water availability are different. Increasing electricity export from northwestern provinces is mainly supported by coal power plants located in extremely arid areas such as the sparsely populated Gobi Desert, leading to large volumetric and stress-weighted virtual water exports (Fig. 6). In contrast, southwestern provinces are water-rich and a large proportion of electricity is generated by hydropower whose water use is not included in this study. However, hydropower dams can have other potential negative impacts including habitat fragmentation (Cooper et al., 2016), altered timing of streamflow relative to environmental needs (Richter and Thomas, 2007), and increasing vulnerability to water shortages (Di Baldassarre et al., 2018) which also need to be considered in planning at the electricity-water nexus.

3.3. Driving forces of changes in virtual water transfer

Different driving forces behind the changing virtual water transfer network are identified using LMDI decomposition (Section 2.2). Growth in electricity demand and increases in the share of imported electricity are the two primary factors that drove the increase in the gross volume of virtual water transfers, and this growth was partially offset by water efficiency improvements of thermal power generation and the increasing share of renewable electricity (Fig. 9). The cumulative contribution of demand growth amounted to $381 \times 10^6 \text{ m}^3$, accounting for 60% of the cumulative increase from 2006 to 2016. The other 40% of the observed increase

($256 \times 10^6 \text{ m}^3$) was attributed to the increasing share of imported electricity. The largest factor contributing to reduced virtual water flows was improvement in water consumption efficiency of thermal power generation, contributing $214 \times 10^6 \text{ m}^3$ of cumulative water conservation and accounting for 55% of the total negative changes. This was achieved by a variety of water conservation countermeasures implemented in China's thermal power sector including adopting air-cooling technologies in arid areas, improving in-plant water reuse and recycling, as well larger generating units with higher efficiency (Zhang et al., 2016b). However, this effect mainly took place before 2012 and the rate of water efficiency improvements has slowed in recent years due to diminishing water conservation potential in traditional coal power plants (Zhang et al., 2018). Renewable electricity penetration also led to water conservation co-benefits. Cumulative contribution of electricity mix changes amounted to $144 \times 10^6 \text{ m}^3$, and its effect increased after 2012 when the share of hydro, wind and solar power started to grow quickly (Fig. 9). The effect of electricity transmission structure was relatively small compared to other factors, which slightly increased virtual water transfer volumes before 2012 and slightly reduced virtual water transfer volumes after then.

For scarce virtual water transfer, the conservation effect of decreasing scarce water consumption intensity was even larger. Improvements in the water intensity of thermoelectric power generation cumulatively reduced scarce virtual water transfer by $146 \times 10^6 \text{ m}^3$, accounting for 81% of the total negative changes (Fig. 9b). Since provinces under higher water stress dominate the scarce virtual water network (Fig. 8), this result implies that water efficiency of thermal power generation has improved more in water-stressed regions than in water-rich regions. There is a negative correlation between the average WSI values of thermal power generation (representing the average water stress level of the locations for thermal power generation) and changes in the average thermoelectric water consumption intensity (Fig. 10). For most provinces in North China Grid and Northwest China Grid under high water stress, average water consumption factors decreased by more than $0.5 \text{ m}^3/\text{MWh}$ from 2006 to 2016 (Fig. 10a), similar to scarce water consumption factors (Fig. 10b). In contrast, the average water consumption factor increased in some provinces with very low WSI values in Central China Grid and South China Grid. This is mainly due to the increased proportion of recirculating

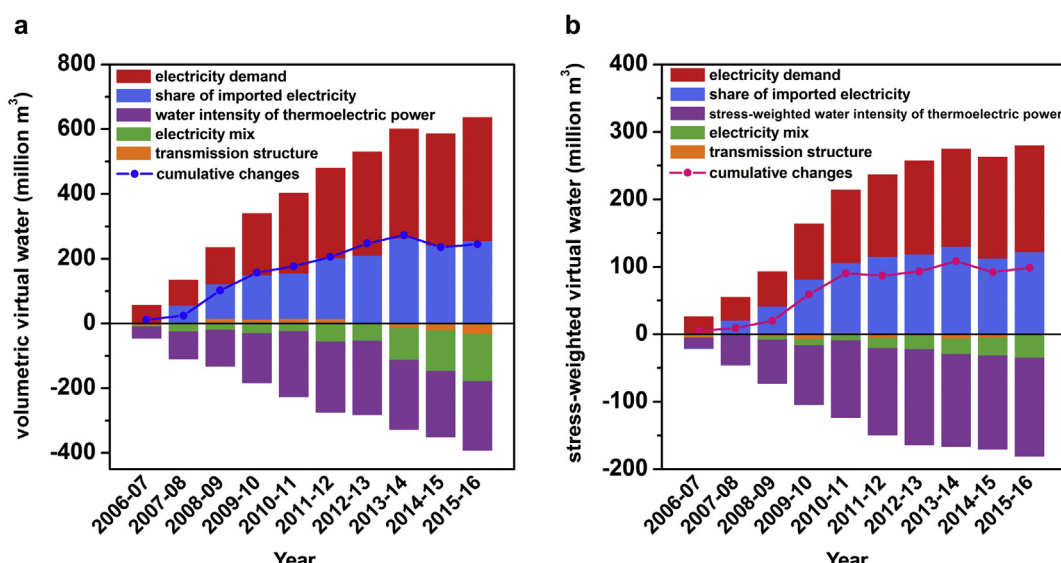


Fig. 9. Decomposition of driving forces for volumetric virtual water (a) and stress-weighted virtual water (b) transfers.

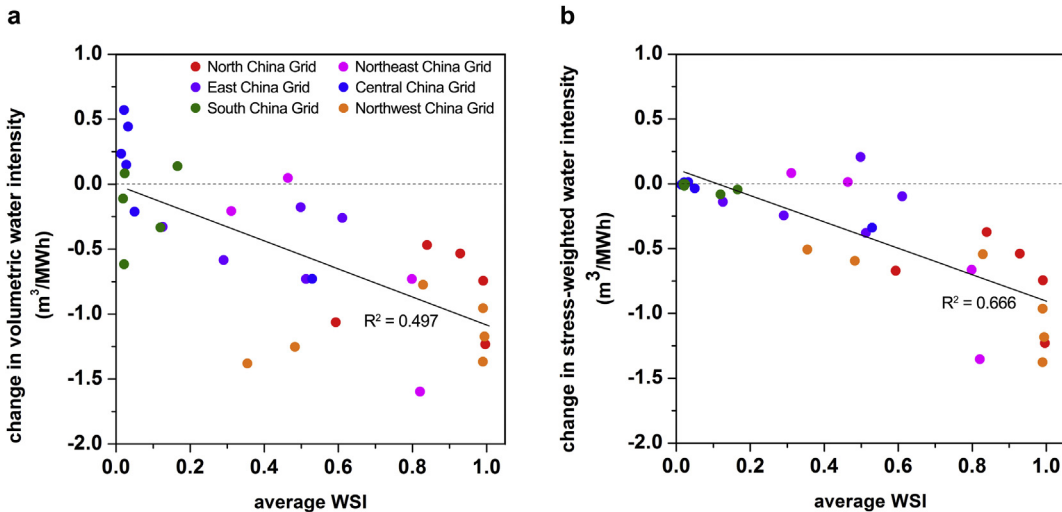


Fig. 10. Changes in water intensity of thermoelectric power over different water stress levels.

cooling plants, which have higher water consumption factors, substituting for once-through cooling plants. After adjustment, changes in stress-weighted water consumption factor in water-rich regions are close to zero. Some key provinces in the virtual water transfer network such as Hubei, Hunan, and Chongqing have increased water consumption factors, but stress-weighted water consumption factors decreased in almost all key provinces in the virtual scarce water transfer network. Different changes in water intensities measured by physical volumes and scarcity-adjusted volumes contribute to the relatively lower growth of the total virtual scarce water transfer (increased by 45%) than the total virtual water transfer (increased by 51%).

4. Discussion

This section is divided into three sub-sections. Section 4.1 discusses China's policies affecting the virtual water network. Section 4.2 addresses the implications for water conservation in China's power sector. Section 4.3 explores the advantages and limitations of this study.

4.1. Policies affecting the virtual water network

Multiple policies in China's power sector affected the evolution of the virtual water network. The decomposition analysis identified the increasing share of imported electricity is a major factor resulting in the growing volume of virtual water transfers (Fig. 9). This is a direct consequence of the West-to-East electricity transmission strategy. In China's 11th-Five-Year plan (2006–2010) for energy development, five western provinces were listed as key regions for construction of large coal power bases, including Shanxi, Shaanxi, Inner Mongolia, Guizhou and Yunnan (NDRC, 2007). Xinjiang was added to this list in the 12th-Five-Year plan (2011–2015) for energy development (State Council, 2013). The latter plan also required that new coal power production should be highly restricted in eastern city agglomerations including the Beijing-Tianjin-Hebei region, Yangtze River Delta, and Pearl River Delta.

Decreasing water intensity of thermal power generation is the most important factor that reduced the virtual water transfers. This can be attributed to various water conservation policies in China's power sector. Zhang et al. (2018) show that the overall water efficiency improvements of thermal power generation in China can be

explained by three types of policies. First, regulations on cooling technology selection led to rapid diffusion of low-freshwater-intensity air-cooling in northwestern regions (NDRC, 2004) and seawater cooling in coastal regions (NDRC, 2005). Second, technological requirements for newly built plants mandated adoption of large units (300 MW or larger) with higher water efficiency (NDRC, 2007). Third, more stringent water withdrawal standards (GAQSIQ and SAC, 2012) and water withdrawal permitting system (State Council, 2006) that promote water conservation technologies (MIIT et al., 2013). These policies have significantly contributed to the decoupling between water use and thermoelectric power generation in China since 2000 (Fig. 9).

The role of electricity mix changes became significant after 2010 (Fig. 9). In the 12th-Five-Year Plan for energy development (State Council, 2013), expected targets for wind power and solar PV capacities were first introduced, which reflects China's determination to develop renewable energy capacity. Deployment of wind and solar PV power in major electricity exporting provinces in the western regions was accelerated during the 12th-Five-Year period. Electricity generation by wind and solar PV power reached 307 TWh in 2016 (5.1% of the national total), more than six times greater than in 2010. Hydropower generation also grew by 71% from 2010 through 2016, compared to 27% growth in thermal power generation.

4.2. Implications for water conservation in China's power sector

Importing electricity from inland western regions to eastern coastal provinces can alleviate local water stress in these load centers, especially for the Beijing-Tianjin-Hebei and Yangtze River Delta regions, in addition to co-benefits such as improved air quality (Ling et al., 2019). However, due to the mismatch between coal resources and water resources in the main western exporting provinces, the growing amount of long-distance electricity transmission has geographically shifted the burden of water stress. This study is the first to reveal the historical trend of water stress shift at the provincial resolution in China. The growing spatial disconnect between urban virtual water importers and rural virtual water exporters may exacerbate challenges in water scarce areas when satisfying consumers' welfare in the densely populated areas is given more priority than conserving scarce natural resources in the remote areas (Zhang et al., 2019).

The shifts in virtual water transfers through time in this study are

occurring concurrent to climate and land use-driven hydrological changes including changes in groundwater recharge (Hyndman et al., 2017) and water withdrawals for urban consumption (Garrick et al., 2019), and agriculture's expanding footprint and water use (Gao et al., 2016). Many of the virtual water exporting areas have significant and well-documented hydrological challenges (Aeschbach-Hertig and Gleeson, 2012). For example, the Hebei province exports significant virtual water to Beijing but both are part of the highly stressed North China Plain region, a critical food-producing area with significant groundwater depletion challenges (Cao et al., 2013). Increasing water consumption associated with expanding energy production in the Hebei province may exacerbate existing inter-sectoral conflict in the region (Kendy et al., 2007). Other water scarce regions with significant virtual water exports identified in this analysis have significant local water use which is likely to be challenged by expanding electricity production. For instance, Inner Mongolia contains substantial irrigated agriculture which relies on both surface water and groundwater (Wu et al., 2015) and has numerous groundwater-dependent ecosystems (Zhu et al., 2012) but exports significant virtual water to Beijing and Liaoning (Figs. 7 and 8). Similarly, Xinjiang (Han et al., 2015) and Ningxia (Xu et al., 2013) are major virtual water exporters with local surface water and groundwater-dependent agriculture.

Given these competing energy, urban, and agricultural demands on water resources, the results of this study suggest that policies must integrate across the entire food-energy-water nexus at both local and regional scales (D'Odorico et al., 2018). Although water conservation measures have been implemented at the individual plant level, system-level integrated planning across the electricity-water nexus (Khan et al., 2018) has not yet been implemented in China. For example, the latest government report on potential risks for coal power planning and construction considers the northwestern provinces to be unconstrained by environmental and water resources (NEA (National Energy Administration), 2019), despite the high water stress in most coal mining and coal power industrial agglomerations in Xinjiang, Inner Mongolia, and Ningxia (Fig. 1; Zhang et al., 2016b). Concurrently, China's new, more stringent water resources management system took effect in 2012 (State Council, 2012) and introduced caps for national total freshwater withdrawals. Balancing these competing water users will require cross-sectoral policies that integrate traditional energy planning, land planning, and water resources management agencies (Scanlon et al., 2017).

This study highlights a major synergistic opportunity at the water-energy nexus: policies for decarbonizing China's power system have strong co-benefits with water conservation. The decomposition analysis showed that the increasingly diverse electricity mix including more renewable sources such as wind and solar PV power has partially counteracted increases in stress-weighted virtual water transfers, while the water efficiency improvements of coal power generation are diminishing (Fig. 9). Since the west-to-east electricity transmission capacity is targeted to increase from 140 GW in 2015 to 270 GW (13.5% of national total power capacity) by 2020 (NDRC, 2017), water stress may increase in western regions if this new capacity is dominated by thermoelectric power generation. Instead, this study shows that incorporating large proportions of wind and solar PV power can help meet this need while potentially decreasing water stress if thermoelectric power generation is reduced during this period. This encourages China to accelerate deeply decarbonizing for the sustainable development goals (McCollum et al., 2018).

4.3. Advantages and limitations of this study

This study constructed time-series inter-provincial electricity

transmission matrices based on physical, rather than economic, units. Compared to previous studies using monetary MRIO tables (e.g., Zhang and Anadon, 2013), physical unit accounting can avoid inherent shortcomings of monetary input-output analysis such as sector aggregation bias (Piñeroa et al., 2015) and price inhomogeneity (Weiss and Duchin, 2006). However, some indicators covered by previous studies are not included in this one, such as the water footprint of hydropower and grey water footprints (Liao et al., 2019). This study does not account for potential negative impacts (Madden et al., 2013) or risks (Logan and Stillwell, 2018) of power plants on aquatic communities via thermal pollution, nor does it consider evaporation from reservoirs as consumptive water use by hydropower generation which significantly increases virtual water exports from the water-abundant Central China Grid (Guo et al., 2016a). However, previous studies considering hydropower evaporation have substantially lower spatial resolution (regional rather than provincial), shorter time periods (at most 6 years), and lower data quality (top-down estimation of water use). This study is based on a time-series bottom-up water use inventory of thermoelectric power generation in China (Zhang et al., 2018) and water stress map at the catchment resolution. The higher data quality in the present study enabled more accurate calculation of stress-weighted volumes of water consumption and mapping of both electricity and virtual water transfers at the provincial resolution. Large differences between the volumetric and stress-weighted virtual water networks reflect significant heterogeneity in the spatial distribution of both water scarcity and electricity production in China, and highlights the need for the high-resolution, bottom-up methods presented here.

5. Conclusions

This study reveals the historical trend of the virtual water transfers embodied in inter-provincial electricity transmission in China and quantify significant scale and structural changes of the virtual water networks. First, electricity production hubs and load centers were increasingly separated from each other in China, which results in a growing west-to-east virtual water transfer pattern. Second, stress-weighted virtual water export from water-deficient northwestern provinces increased tremendously during the past decade, primarily as a result of rapid development of coal power capacity. Electricity consumption in the Beijing-Tianjin-Hebei region and Shandong is responsible for large volumes of scarce water consumption in West Inner Mongolia and Ningxia, and virtual water flow from Xinjiang to Henan is the fastest-growing stress-weighted virtual water link in the network. Third, thanks to water conservation policies in the power sector and rising shares of renewable electricity in western provinces, the volumes of volumetric and stress-weighted virtual water transfers grew much slower than the amount of inter-provincial electricity transmission. Given that the potential of water efficiency improvements of traditional coal power generation has been diminishing since 2012, this indicates that increasing wind and solar PV power capacity should be prioritized due to water conservation and decarbonization synergy. Facing the trend of increasing west-to-east electricity transmission scale in the future, water scarcity should be explicitly accounted for in integrated system-wide electricity planning, and further renewable electricity development can bring carbon and hydrological co-benefits by alleviating water stress caused by electricity export in the northwestern regions.

Acknowledgements

This study is supported by National Natural Science Foundation of China (Grant number 71503182) and the Fundamental Research

Funds for the Central Universities. Chao Zhang is also supported by the research fund from Covestro-Tongji Chair for Sustainable Development.

References

- Aeschbach-Hertig, W., Gleeson, T., 2012. Regional strategies for the accelerating global problem of groundwater depletion. *Nat. Geosci.* 5, 853–861.
- Allan, J.A., 1998. Virtual water: a strategic resource, global solutions to regional deficits. *Gr. Water* 36, 545–546.
- Ang, B.W., 2005. The LMDI approach to decomposition analysis: a practical guide. *Energy Policy* 33, 867–871.
- Averyt, K., Macknick, J., Rogers, J., Madden, N., Fisher, J., Meldrum, J., Newmark, R., 2013. Water use for electricity in the United States: an analysis of reported and calculated water use information for 2008. *Environ. Res. Lett.* 8, 015001.
- Behrens, P., van Vliet, M.T.H., Nanninga, T., Walsh, B., Rodrigues, J.F.D., 2017. Climate change and the vulnerability of electricity generation to water stress in the European Union. *Nat. Energy* 2, 17114.
- Cao, G., Zheng, C., Scanlon, B.R., Liu, J., Li, W., 2013. Use of flow modeling to assess sustainability of groundwater resources in the North China Plain. *Water Resour. Res.* 49, 159–175.
- CEC (China Electricity Council), 2000-2015. Annual Compilation of Statistics of Power Industry [in Chinese]. China Electricity Council (CEC), Beijing.
- CEC (China Electricity Council), 2018. Annual Report of Chinese Electric Power Industry 2018. China Market Press, Beijing ([in Chinese]).
- Chen, Q., Kang, C., Ming, H., Wang, Z., Xia, Q., Xu, G., 2014. Assessing the low-carbon effects of inter-regional energy delivery in China's electricity sector. *Renew. Sustain. Energy Rev.* 32, 671–683.
- Chini, C.M., Djehdian, L.A., Lubega, W.N., Stillwell, A.S., 2018. Virtual water transfers of the US electric grid. *Nat. Energy* 3, 1115–1123.
- Cooper, A.R., Infante, D.M., Wehrly, K.E., Wang, L., Brenden, T.O., 2016. Identifying indicators and quantifying large-scale effects of dams on fishes. *Ecol. Indicat.* 61, 646–657.
- Di Baldassarre, G., Wanders, N., AghaKouchak, A., Kuil, L., Rangecroft, S., Veldkamp, T.I.E., Garcia, M., Oel, P.R., van Breinl, K., Loon, A.F.V., 2018. Water shortages worsened by reservoir effects. *Nat. Sustain.* 1, 617–622.
- D'Odorico, P., Davis, K.F., Rosa, L., Carr, J.A., Chiarelli, D., Dell'Angelico, J., Gephart, J., MacDonald, G.K., Seekell, D.A., Suweis, S., Rulli, M.C., 2018. The global food-energy-water nexus. *Rev. Geophys.* 56, 456–531.
- Editorial Board, 2015. China Electric Power Yearbook 2006–2016. China Electric Power Press, Beijing ([in Chinese]).
- Feng, K., Hubacek, K., Siu, Y.L., Li, X., 2014. The energy and water nexus in Chinese electricity production: a hybrid life cycle analysis. *Renew. Sustain. Energy Rev.* 39, 342–355.
- Gao, Z., Zhang, L., Zhang, X., Cheng, L., Potter, N., Cowan, T., Cai, W., 2016. Long-term streamflow trends in the middle reaches of the Yellow River Basin: detecting drivers of change. *Hydrol. Process.* 30, 1315–1329.
- GAQSIQ (General Administration of Quality Supervision Inspection and Quarantine), SAC (Standardization Administration Commission), 2012. Norm of Water Intake - Part 1: Fossil Fired Power Production. GB/T 18916.1-2012. [in Chinese].
- Garrison, D., Stefano, L.D., Yu, W., Jorgensen, I., O'Donnell, E., Turley, L., Aguilera-Barajas, I., Dai, X., Leão, R. de S., Punjabi, B., Schreiner, B., Svensson, J., Wight, C., 2019. Rural water for thirsty cities: a systematic review of water reallocation from rural to urban regions. *Environ. Res. Lett.* 14, 043003.
- Guo, R., Zhu, X., Chen, B., Yue, Y., 2016a. Ecological network analysis of the virtual water network within China's electric power system during 2007–2012. *Appl. Energy* 168, 110–121.
- Guo, Z., Ma, L., Liu, P., Jones, I., Li, Z., 2016b. A multi-regional modelling and optimization approach to China's power generation and transmission planning. *Energy* 116, 1348–1359.
- Han, M., Zhao, C., Šimunek, J., Feng, G., 2015. Evaluating the impact of groundwater on cotton growth and root zone water balance using Hydrus-1D coupled with a crop growth model. *Agric. Water Manag.* 160, 64–75.
- He, G., Kammen, D.M., 2014. Where, when and how much wind is available? A provincial-scale wind resource assessment for China. *Energy Policy* 74, 116–122.
- He, G., Kammen, D.M., 2016. Where, when and how much solar is available? A provincial-scale solar resource assessment for China. *Renew. Energy* 85, 74–82.
- Hoekstra, A.Y., Chapagain, A.K., Aldaya, M.M., Mekonnen, M.M., 2011. The Water Footprint Assessment Manual: Setting the Global Standard. Earthscan, London.
- Hyndman, D.W., Xu, T., Deines, J.M., Cao, G., Nagelkirk, R., Viña, A., McConnell, W., Basso, B., Kendall, A.D., Li, S., Luo, L., Lupi, F., Ma, D., Winkler, J.A., Yang, W., Zheng, C., Liu, J., 2017. Quantifying changes in water use and groundwater availability in a megacity using novel integrated systems modeling. *Geophys. Res. Lett.* 44, 8359–8368.
- Kendy, E., Wang, J., Molden, D.J., Zheng, C., Liu, C., Steenhuis, T.S., 2007. Can urbanization solve inter-sector water conflicts? Insight from a case study in Hebei Province, North China Plain. *Water Policy* 9, 75–93.
- Khan, Z., Linares, P., Rutten, M., Parkinson, S., Johnson, N., García-González, J., 2018. Spatial and temporal synchronization of water and energy systems: towards a single integrated optimization model for long-term resource planning. *Appl. Energy* 210, 499–517.
- Li, F., Xiao, X., Xie, W., Ma, D., Song, Z., Liu, K., 2018. Estimating air pollution transfer by interprovincial electricity transmissions: the case study of the Yangtze River Delta Region of China. *J. Clean. Prod.* 183, 56–66.
- Liao, X., Hall, J.W., Eyre, N., 2016. Water use in China's thermoelectric power sector. *Glob. Environ. Chang.* 41, 142–152.
- Liao, X., Chai, L., Xu, X., Lu, Q., Ji, J., 2019. Grey water footprint and interprovincial virtual grey water transfers for China's final electricity demands. *J. Clean. Prod.* 227, 111–118.
- Lindner, S., Liu, Z., Guan, D., Geng, Y., Li, X., 2013. CO₂ emissions from China's power sector at the provincial level: consumption versus production perspectives. *Renew. Sustain. Energy Rev.* 19, 164–172.
- Ling, Z., Huang, T., Li, J., Zhou, S., Lian, L., Wang, J., Zhao, Y., Mao, X., Gao, H., Ma, J., 2019. Sulfur dioxide pollution and energy justice in Northwestern China embodied in West-East Energy Transmission of China. *Appl. Energy* 238, 547–560.
- Liu, M., Huang, Y., Ma, Z., Jin, Z., Liu, X., Wang, H., Liu, Y., Wang, J., Jantunen, M., Bi, J., Kinney, P.L., 2017. Spatial and temporal trends in the mortality burden of air pollution in China: 2004–2012. *Environ. Int.* 98, 75–81.
- Logan, L.H., Stillwell, A.S., 2018. Probabilistic assessment of aquatic species risk from thermoelectric power plant effluent: incorporating biology into the energy-water nexus. *Appl. Energy* 210, 434–450.
- Madden, N., Lewis, A., Davis, M., 2013. Thermal effluent from the power sector: an analysis of once-through cooling system impacts on surface water temperature. *Environ. Res. Lett.* 8, 035006.
- McCollum, D.L., Zhou, W., Bertram, C., De Boer, H.S., Bosetti, V., Busch, S., Despres, J., Drouet, L., Emmerling, J., Fay, M., Fricko, O., Fujimori, S., Gidden, M., Harmsen, M., Huppmann, D., Iyer, G., Krey, V., Kriegler, E., Nicolas, C., Pachauri, S., Parkinson, S., Poblete-Cazenave, M., Rafaj, P., Rao, N., Rosenberg, J., Schmitz, A., Schoepf, W., van Vuuren, D., Riahi, K., 2018. Energy investment needs for fulfilling the Paris agreement and achieving the sustainable development goals. *Nat. Energy* 3, 589–599.
- McMahon, J.E., Price, S.K., 2011. Water and energy interactions. *Annu. Rev. Environ. Resour.* 36, 163–191.
- MIIT (Ministry of Industry and Information Technology), 2013. MWR (Ministry of water resources), NBS (national Bureau of Statistics), NWCO (national water conservation office). Water efficiency guide for key industrial sectors [in Chinese]. Retrieved 2019/09/01 from. www.miit.gov.cn/n1146295/n1652858/n1652930/n3757016/c3762100/content.html.
- NDRC (National Development and Reform Commission), 2004. Requirements by the National Development and Reform Commission on the planning and construction of coal power plants [in Chinese]. Retrieved 2019/09/01 from. www.nea.gov.cn/2012-01/04/c_131262602.htm.
- NDRC (National Development and Reform Commission), 2005. SOA (state oceanic administration), MOF (Ministry of finance). National development plan of seawater utilization [in Chinese]. Retrieved 2019/09/01 from. www.sdpc.gov.cn/zcfb/zcfbghwhb/200510/t20051013_579674.htm.
- NDRC (National Development and Reform Commission), 2007. The 11th-five-year (2006–2010) plan for energy development. plants [in Chinese]. Retrieved 2019/09/01 from. www.nea.gov.cn/2007-04/11/c_131215360.htm.
- NDRC (National Development and Reform Commission), 2017. The 13th five-year (2016–2020) development plan for electric power industry [in Chinese]. Retrieved 2019/09/01 from. www.ndrc.gov.cn/zcfb/zcfbghwhb/201612/P020161222570036010274.pdf.
- NEA (National Energy Administration), 2019. Notification by National Energy Administration on risk warning for coal power planning and construction in 2022 [in Chinese]. Retrieved 2019/09/01 from. zfxgk.nea.gov.cn/auto84/201904/t20190419_3655.htm.
- Pfister, S., Koehler, A., Hellweg, S., 2009. Assessing the environmental impacts of freshwater consumption in LCA. *Environ. Sci. Technol.* 43, 4098–4104.
- Piñeroa, P., Heikkilä, M., Mäenpää, I., Pongrácz, E., 2015. Sector aggregation bias in environmentally extended input output modeling of raw material flows in Finland. *Ecol. Econ.* 119, 217–229.
- Qu, S., Li, Y., Liang, S., Yuan, J., Xu, M., 2018. Virtual CO₂ emission flows in the global electricity trade network. *Environ. Sci. Technol.* 52, 6666–6675.
- Richter, B., Thomas, G., 2007. Restoring environmental flows by modifying dam operations. *Ecol. Soc.* 12, 12.
- Scanlon, B.R., Ruddell, B.L., Reed, P.M., Hook, R.J., Zheng, C., Tidwell, V.C., Siebert, S., 2017. The food-energy-water nexus: transforming science for society. *Water Resour. Res.* 53, 3550–3556.
- State Council, 2006. Regulations on water withdrawal permits and water resource fee collection [in Chinese]. Retrieved 2019/09/01 from. www.gov.cn/zwgk/2006-03/06/content_220023.htm.
- State Council, 2012. Opinions of the state Council on implementing the most stringent water resource management system [in Chinese]. Retrieved 2019/09/01 from. www.gov.cn/zwgk/2012-02/16/content_2067664.htm.
- State Council, 2013. The 12th-five-year (2011–2015) plan for energy development [in Chinese]. Retrieved 2019/09/01 from. www.gov.cn/zwgk/2013-01/23/content_2318554.htm.
- State Council, 2014. Action plan for energy development strategy (2014–2020) [in Chinese]. Retrieved 2019/09/01 from. www.gov.cn/zhengce/content/2014-11-19/content_9222.htm.
- van Vliet, M.T.H., Wiberg, D., Leduc, S., Riahi, K., 2016. Power-generation system vulnerability and adaptation to changes in climate and water resources. *Nat. Clim. Chang.* 6, 375–380.
- Wada, Y., Graaf, I.E.M.d., Beek, L.P.H.v., 2016. High-resolution modeling of human and climate impacts on global water resources. *J. Adv. Model. Earth Syst.* 8,

- 735–763.
- Wang, X., Lu, Z., 2018. All Ultra-high Voltage Electricity Transmission Projects for Air Pollution Control Have Been Completed. China Energy Newspaper, Beijing.
- Wang, J., Zhong, L., Long, Y., 2016. Baseline Water Stress: China. World Resources Institute, Beijing.
- Wang, H., Wang, W., Liang, S., Zhang, C., Qu, S., Liang, Y., Li, Y., Xu, M., Yang, Z., 2019. Determinants of greenhouse gas emissions from interconnected grids in China. *Environ. Sci. Technol.* 53, 1432–1440.
- Wei, W., Wu, X., Li, J., Jiang, X., Zhang, P., Zhou, S., Zhu, H., Liu, H., Chen, H., Guo, J., Chen, G., 2018. Ultra-high voltage network induced energy cost and carbon emissions. *J. Clean. Prod.* 178, 276–292.
- Weisz, H., Duchin, F., 2006. Physical and monetary input-output analysis: what makes the difference? *Ecol. Econ.* 57, 534–541.
- Wu, Y., Liu, T., Paredes, P., Duan, L., Pereira, L.S., 2015. Water use by a groundwater dependent maize in a semi-arid region of Inner Mongolia: evapotranspiration partitioning and capillary rise. *Agric. Water Manag.* 152, 222–232.
- Xu, X., Huang, G., Sun, C., Pereira, L.S., Ramos, T.B., Huang, Q., Hao, Y., 2013. Assessing the effects of water table depth on water use, soil salinity and wheat yield: searching for a target depth for irrigated areas in the upper Yellow River basin. *Agric. Water Manag.* 125, 46–60.
- Zeng, M., Peng, L., Fan, Q., Zhang, Y., 2016. Trans-regional electricity transmission in China: status, issues and strategies. *Renew. Sustain. Energy Rev.* 66, 572–583.
- Zhang, C., Anadon, L.D., 2013. Life cycle water use of energy production and its environmental impacts in China. *Environ. Sci. Technol.* 47, 14459–14467.
- Zhang, C., Zhong, L., Fu, X., Wang, J., Wu, Z., 2016a. Revealing water stress by the thermal power industry in China based on a high spatial resolution water withdrawal and consumption inventory. *Environ. Sci. Technol.* 50, 1642–1652.
- Zhang, C., Zhong, L., Fu, X., Zhao, Z., 2016b. Managing scarce water resources in China's coal power industry. *Environ. Manag.* 57, 1188–1203.
- Zhang, C., Zhong, L., Liang, S., Sanders, K.T., Wang, J., Xu, M., 2017a. Virtual scarce water embodied in inter-provincial electricity transmission in China. *Appl. Energy* 187, 438–448.
- Zhang, X., Liu, J., Tang, Y., Zhao, X., Yang, H., Gerbens-Leenes, P.W., van Vliet, M.T.H., Yan, J., 2017b. China's coal-fired power plants impose pressure on water resources. *J. Clean. Prod.* 161, 1171–1179.
- Zhang, C., Zhong, L., Wang, J., 2018. Decoupling between water use and thermoelectric power generation growth in China. *Nat. Energy* 3, 792–799.
- Zhang, Q., Nakatani, J., Shan, Y., Moriguchi, Y., 2019. Inter-regional spillover of China's sulfur dioxide (SO_2) pollution across the supply chains. *J. Clean. Prod.* 207, 418–431.
- Zheng, X., Wang, C., Cai, W., Kummu, M., Varis, O., 2016. The vulnerability of thermoelectric power generation to water scarcity in China: current status and future scenarios for power planning and climate change. *Appl. Energy* 171, 444–455.
- Zhou, K., Yang, S., Shen, C., Ding, S., Sun, C., 2015. Energy conservation and emission reduction of China's electric power industry. *Renew. Sustain. Energy Rev.* 45, 10–19.
- Zhou, Y., Li, H., Wang, K., Bi, J., 2016. China's energy-water nexus: spillover effects of energy and water policy. *Glob. Environ. Chang.* 40, 92–100.
- Zhu, J., Yu, J., Wang, P., Zhang, Y., Yu, Q., 2012. Interpreting the groundwater attributes influencing the distribution patterns of groundwater-dependent vegetation in northwestern China. *Ecohydrology* 5, 628–636.
- Zhu, X., Guo, R., Chen, B., Zhang, J., Hayat, T., Alsaedi, A., 2015. Embodiment of virtual water of power generation in the electric power system in China. *Appl. Energy* 151, 345–354.